Thermohydraulic Simulation Of The ITER Magnet System

The problem of complex thermohydraulic simulation of the ITER magnet system using a VINCENTA modelling is discussed. The results of validation of the VINCENTA modelling is presented based on the experiment with the Central Solenoid Model Coil.

Keywords: Superconductivity, Magnet; Cooling system; Thermohydraulic analysis; Numerical simulation.

1. Introduction

For the last seven years, a computer code VINCENTA (registered by the Russian Federation Agency for Patents and Trademarks on Nov. 21, 2002, reg.# 2002611959) has been used for full-scale modelling of the thermo-hydraulic behaviour of the ITER magnet and cryogenic systems. Now its advanced version 5.0 is applied. The simulation capabilities of this code make it possible to construct the general consistent thermal model of the ITER machine on the basis of partial models of its separate components to analyse simultaneously hundreds of parameters for hundreds of components. These 1D and 2D models are used to simulate the transient behaviour of different interconnected ITER components ~~h the~~ taking into account different kinds of their interaction.

Since the results of VINCENTA simulations are used to access the applicability of the engineering solutions and design approaches adopted at the designing stage of ITER project, its validation is of extreme importance. Our experience in applying the VINCENTA modeling to simple systems reveals that the consistency between simulated and experimental results depends strongly on the accuracy of the input data on heat loads and proper choice of some semi-empirical coefficients such as heat transfer, friction factor etc. In the case of complex models, this problem is aggravated due to lack of reliable databases. The testing of the ITER Central Solenoid Model Coil (CSMC) in Japan [1] gave an excellent chance to validate the VINCENTA model similar to the general numerical model applied to simulate the thermo-hydraulics of the ITER magnet system at normal operation.

The cross-section of Central Solenoid Model Coil is shown in figure 1. The main aims of the ITER CSMC testing were to validate all CSMC specifications, to determine the operational limits and to verify the design criteria for the superconducting magnets applied in fusion. About 350 experimental runs were carried out during these tests and more than 400 sensors used to acquire data allowed us to store a considerable amount of information during this test campaign.

A detailed VINCENTA model has been developed to simulate the thermo-hydraulic behaviour of CSMC at pulsed operation with high heat pulses generated in the conducting components of the ITER magnets.

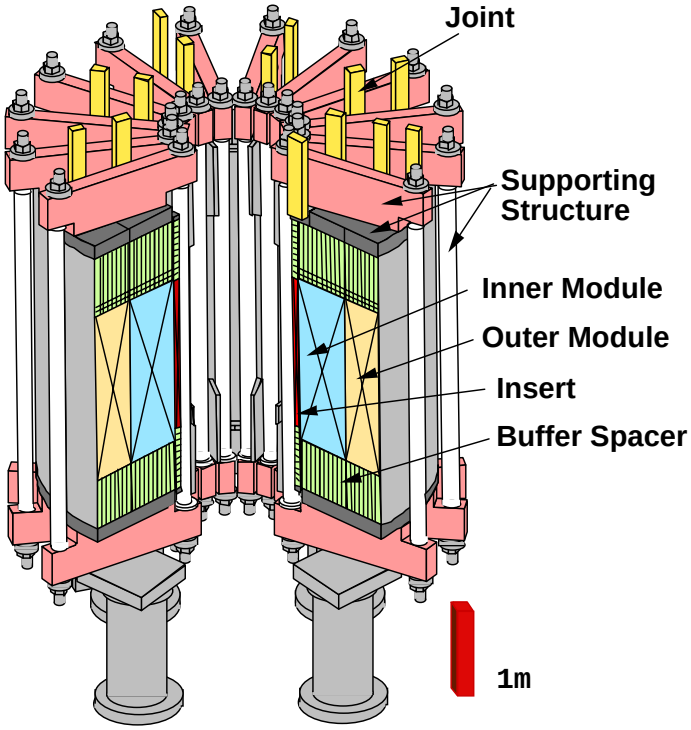

Characteristics	Inner Module		Outer Module
Conductor	CS1	CS2	CS2
Number of layers	4	6	8
Number of turns / layer	31	34	34
Inner radius (ground insul.)	0.790 m		1.367 m
Outer radius (ground insul.)	1.357 m		1.800 m
Height (incld. Buffer zone)	2.795 m		
Maximum operating field	13 T		
Operating current	46 kA		
Stored energy at 13 T	641 MJ		

Figure 1. CSMC assembly.

2. Mathematical model

The CSMC mathematical model is a combination of three partial numerical models:

1. The 1D model used to simulate the transient behaviour of helium flows in different tubes, including the cooling channels of the superconducting cables of inner and outer modules, the Central Solenoid Coil Insert (CSCI), two supercritical helium heat exchangers, the upper and lower support structures, the base, auxiliary cryogenic systems etc. The total number of channels modelled in the 1-D approximation was above 160. Each of 36 superconducting cables-in-conduit conductors (CICC) was modelled separately. In each CICC, two thermodynamically non-equilibrium helium flows were considered: one flowing in the cable space between strands and another within spiral core. Transverse heat and mass transfer between these flows occurred through the gaps between spiral convolution.
2. The 2D difference model used to simulate transient heat exchange conditions over the CSMC cross-section in the cylindrical coordinate system. Thermal inter-turn interaction takes place between turns including the upper and lower support structures. The 2D calculation mesh for 5 cross- sections has over 450,000 nodes. The 2D heat transfer model is combined with the 1D thermo-hydraulic model via consistent boundary conditions for a 2D wetted boundary and the heat load for the 1D flow model.

3. The 2D model used to simulate the alternating current (AC) losses in the CSMC and CSCI conductors based on field maps for different time points of the experiment scenario.

The linkage between the 1D and 2D models is specified taking into account the counter flows in the adjacent layers of winding. Figure 2 shows the cooling scheme and the location and numbering of the cross-sections calculated. The cooling circuit for CSMC consists of 6 parallel loops equipped with control valves at the inlet and outlet. Besides the winding superconductors, the numerical model of CSMC includes a helium centrifugal pump, two SHe (supercritical helium) heat exchangers, *HXP1* and *HXP2,* and two cryolines.

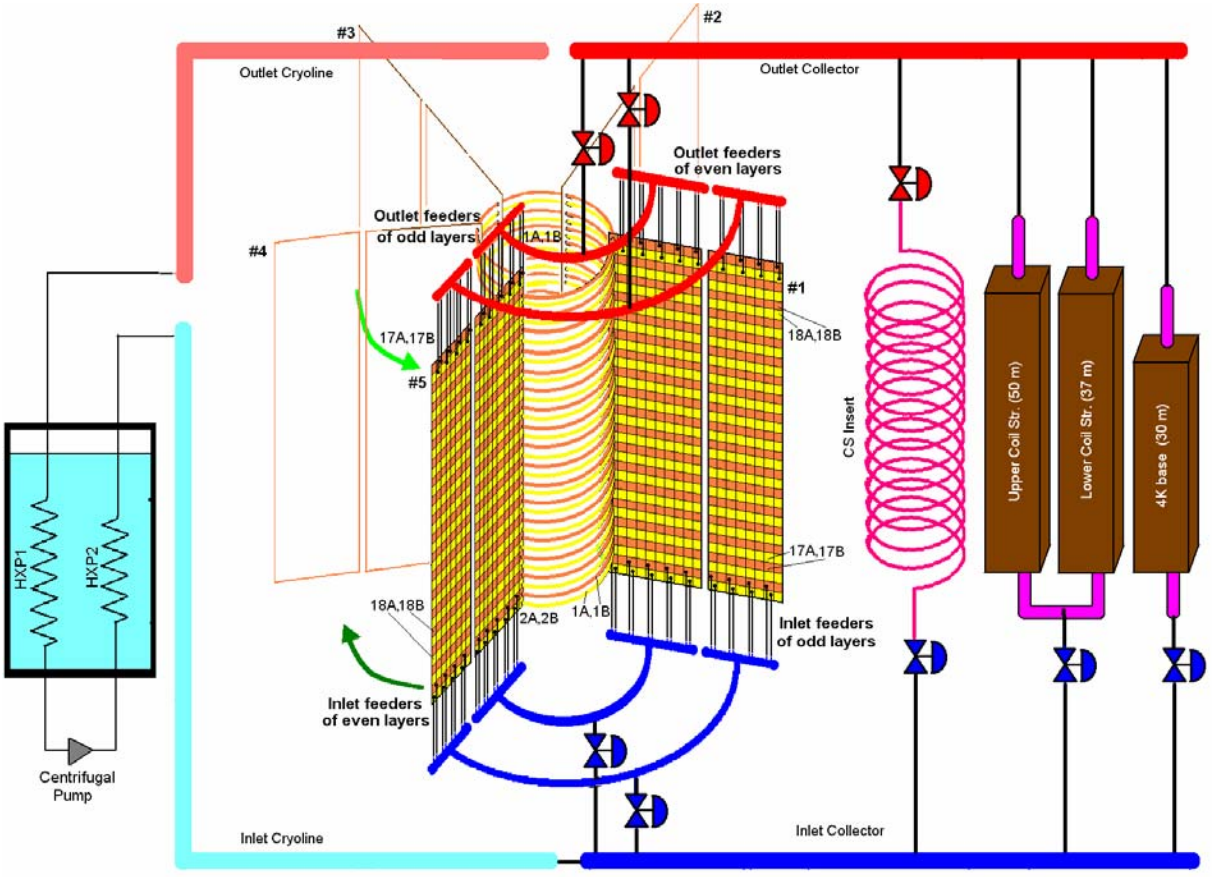

Figure 2. Process flow diagram of the cooling system of CSMC & CSC Insert used for the numerical simulation during current pulses.

3. Initial data

To validate the VINCENTA model the comparison between the data obtained during the CSMC experiment and calculation data was done. During this experiment a series of current pulses with an amplitude increasing from 5 kA up to 46 kA was applied. A series of pulses with currents of 30, 40, 43 and 46 kA on the top taken for simulations and subsequent validation. All pulses were trapezoidal in time, and were repeated with a time interval of about 3000 s, as is shown in figure 3.

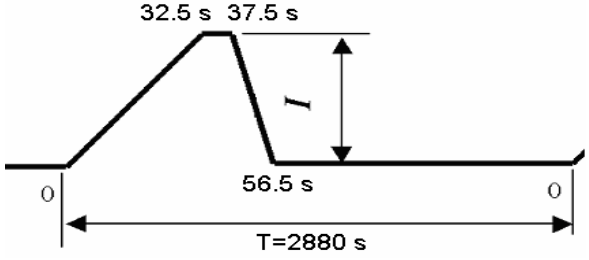

Figure 3. Shape of the current pulses

Before modelling the transient behaviour of CSMC at pulsed operation, some preliminary simulations have been carried out to adjust the initial cooling parameters (helium flow as a function of pressure drop) for 36 conductors, cold valves and cryolines. This important step of simulation was performed with use of the experimental data obtained for the CSMC parameters at static heat loads [2]. Corresponding hydraulic coefficients obtained at this stage of simulations were then used in transient simulations.

At the pulsed operation, CSMC absorbs the AC losses in conductors and coil structures. The model describes complex AC losses over the whole CSMC and CS insert in time and space at varying current. This method allowed the coupling and hysteresis losses in conductors to be determined separately in details. The evaluation of AC losses during current variation was based on the time and space variations in magnetic field B in the conductors of CSMC and CS Insert.

AC losses as a function of space and time are defined from the known correlation equations used for the assessment of the coupling and hysteresis losses in the CIC superconductors [3, 4]. The equations used in the model included a set of parameters to take into account the conductor specifics in different layers, namely $n\tau_L$ and effective filament diameters $D_{\mathrm{eff}L}$. The following approximations were applied in the calculation:

- for the coupling losses in a given layer of winding n_L and conductor turn n_T $P_c(n_L, n_T, t) = \frac{n\tau_L}{\mu_0} A_{st}(n_L)\, \dot{B}(n_L, n_T, t)^2$, W/m,

  where $\dot{B}$ is the time derivative of magnetic field (transversal component) applied to the given layer and turn in time t, T/s; A_{st} is the strand cross section area for the given layer, m^2; μ_0 is the magnetic permeability of vacuum.

- for the hysteresis losses in a given layer of winding n_L and conductor turn n_T due to a change in the transversal field

  $$P_H(n_L, n_T, t) = \frac{2}{3\pi} A_{nonCu}(n_L) \cdot D_{eff}(n_L)\, J_c\big(B(n_L, n_T, t), T(n_L, n_T, t)\big) \dot{B}(n_L, n_T, t),\ \text{W/m},$$

  where $J_c(B,T)$ is the critical current density of Nb_3Sn conductor [5] for a given type of conductor (HPI or HPII); T is the conductor temperature.

The effective filament diameters D_{eff} and parameter $n\tau_L$ were defined individually for each layer of the CSMC winding. The D_{eff} values were specified by the cable manufacturer. Parameters $n\tau_L$ were taken from [6, 7] as initial parameters and then were slightly corrected by the authors to ensure more accurate matching between the calculated data on the evolution of the temperature profile of supercritical helium at the outlet of the conductors and the experimental data obtained for the 46 kA current pulse.

Figures 4 and 5 show integrated coupling and hysteresis losses for the CSMC turns (half of the winding pack) calculated using approximation equations for the 46 kA pulses.

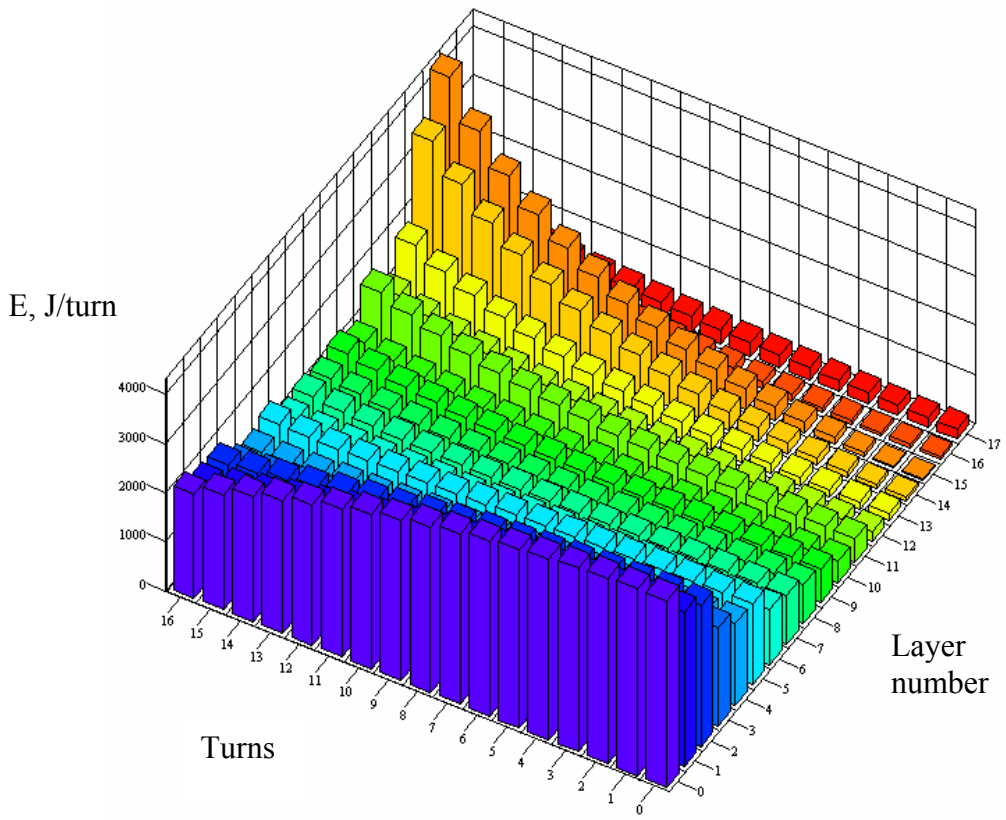

Figure 4. Distribution of coupling losses throughout different turns and layers of CSMC for the 46 kA pulse.

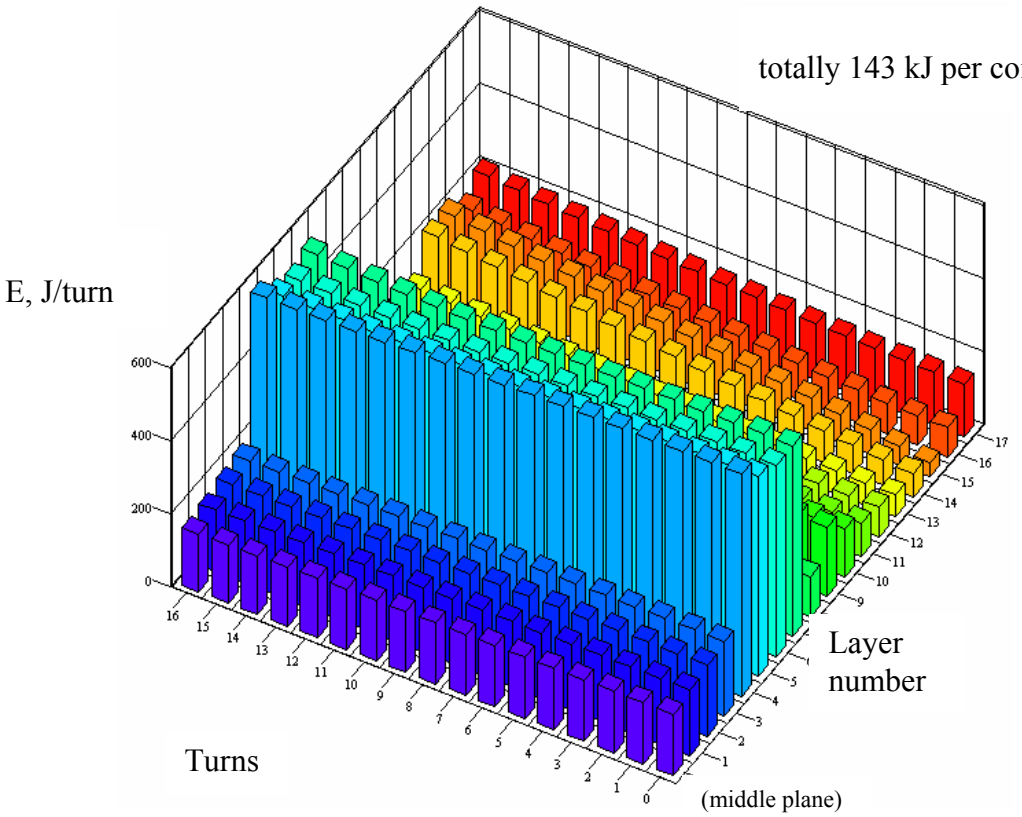

Figure 5. Distribution of hysteresis losses throughout the different turns and layers of CSMC for the 46 kA pulse.

The 1D problem was solved to determine the temperature evolution in the coil structure components. Heat loads in the structures were assumed to be uniformly distributed along the cooling tubes. It was also assumed that eddy current losses in the structures were proportional to $\dot{I}^2$.

4. Comparison between results of numerical simulations and results obtained by the CSMC experiment.

To validate the VINCENTA model, the transient simulations of helium pressure, temperature and mass flow rates were carried out for a series of trapezoid pulses with currents of 30, 40, 43 and 46kA on the flat top.

A comparison between the experiment and numerical simulations was done for the following global and local cooling parameters:

- peaks of helium pressure and temperature in the CSMC cooling loop at the end of each current pulse (global parameters);
- evolution (time- history) of the pressure and temperature after each current pulse at the inlet and outlet of the inner and outer CSMC modules (global parameters);
- evolution of the heat load deposited in the liquid helium (LHe) bath from two heat exchangers with supercritical helium for each current pulse (global parameter);
- evolution (time- histories) of the temperatures and helium flows at the inlet and outlet of each of 36 conductors (local parameters).

The $n\tau$ parameter taken from [6] to calculate the coupling losses in different conductors was then iteratively adjusted in accordance with the evolution of the outlet temperature of the corresponding conductor. It should be mentioned that the outlet temperatures of two conductors (A and B) in each winding layer were different in the experiment. For example, the maximum outlet temperatures in the innermost layer were 6.75K and 7.5K for 1A and 1B conductors, correspondingly. However, it was assumed in the calculations that the average $n\tau$ was identical for both A and B conductors of each winding layer.

4.1 *Temperature variation at the inlet of CSMC*

The experiments have shown that helium temperature varies at the inlet of CSMC during each heat pulse. There are observed two spikes of the inlet helium temperature, namely a short- time spike and a long- time spike. The short- time spike appears during the heat pulse. This spike disappears very rapidly in one minute after each pulse. The short- time spike was predicted by numerical calculations and explained by the total increase in helium pressure in the closed cooling loop of CSMC due to pulsed heat load and the adiabatic compression of helium in the inlet cryoline associated with it.

The long-time spike resulting in a temperature increase of about 0.2K for the 46 kA current pulse disappeared during about 15 minutes after each heat pulse, which was caused by the heat absorbed the LHe bath. As a result, the pressure in the LHe bath increased because the capacity of the cold compressor did not allow the evaporated helium to remove instantly. The constant power cold compressor gradually evacuated the helium evaporated from LHe bath to maintain an initial temperature of 4.4K in the bath and at the inlet of CSMC. During the experiment with pulsed heat loads, the mass flow rate of evaporated helium rises increased by a factor of three compared with the mass flow rate under steady state conditions.

To imitate the changes in the temperature of LHe bath, it was supposed that this temperature varied proportionally to the heat load on the bath. The factor of proportionality between the heat power absorbed by the bath and rise of its temperature was found constant by experiment. The factor was normalized to a 0.2 K increase in the bath temperature for 46 kA pulse. This numerical study has

shown that the temperature spike at the inlet of CSMC disappears in 15 minutes as it was obtained from the experiments. This demonstrates that the changes in the inlet CSMC temperature are due to an increase in the transient pressure in LHe bath.

The above approach to calculate the temperature variations at the CSMC inlet was applied to simulate transient cooling parameters for a series of pulses with different flat top currents of 30 kA, 40 kA, 43 kA and 46 kA. It should be noted that the latest version of the code, VINCENTA 5.0, allows direct simulation of the operation of the cold compressor and the transient behaviour of LHe bath at pulsed heat loads.

4.2 *Global parameters of transient helium flow for a series of current pulses*

Figure 6 shows variations in the helium temperature at the inlet and outlet of CSMC (calculations and experiment). Experimental data were obtained with a time step of 10 s. The data calculated were recorded for characteristic time points shown by open circles. The outlet CSMC temperature is the outlet temperature after mixing the outlet helium flows from six components, namely the inner and outer modules, the low and upper structures and the 4K base. An average deviation between the experiments and the simulations is about 5 % for a series of current pulses. For the 46kA pulse, the maximum outlet temperature is 5.6K by experiment and 5.68K from simulations.

The evolution of the helium pressure at the inlet and outlet of CSMC for the same series of current pulses is shown in figure 7. Good agreement was found between the simulations and experiment. For example, for the 46kA pulse, the peak helium pressure at the CSMC inlet was 0.97 MPa by experiment and 0.98 MPa from simulations.

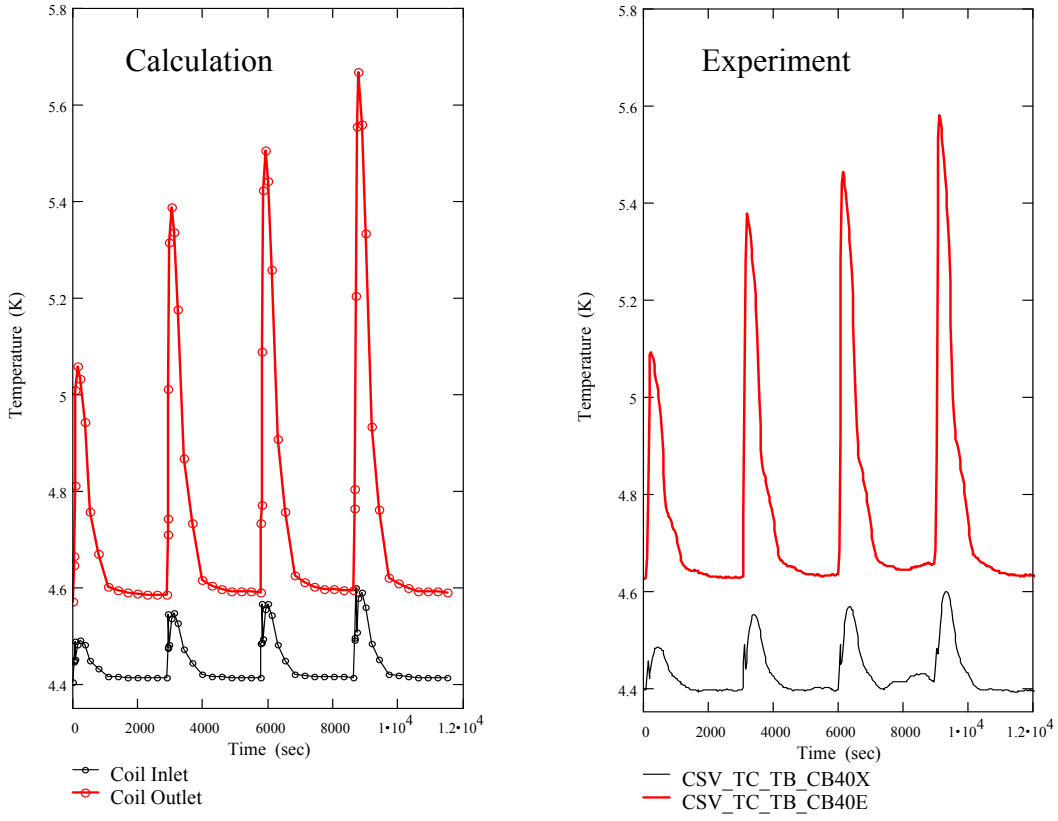

Figure 6. Evolution of temperatures at the inlet and outlet of CSMC for a series of current pulses with amplitudes of 30, 40, 43 and 46 kA.

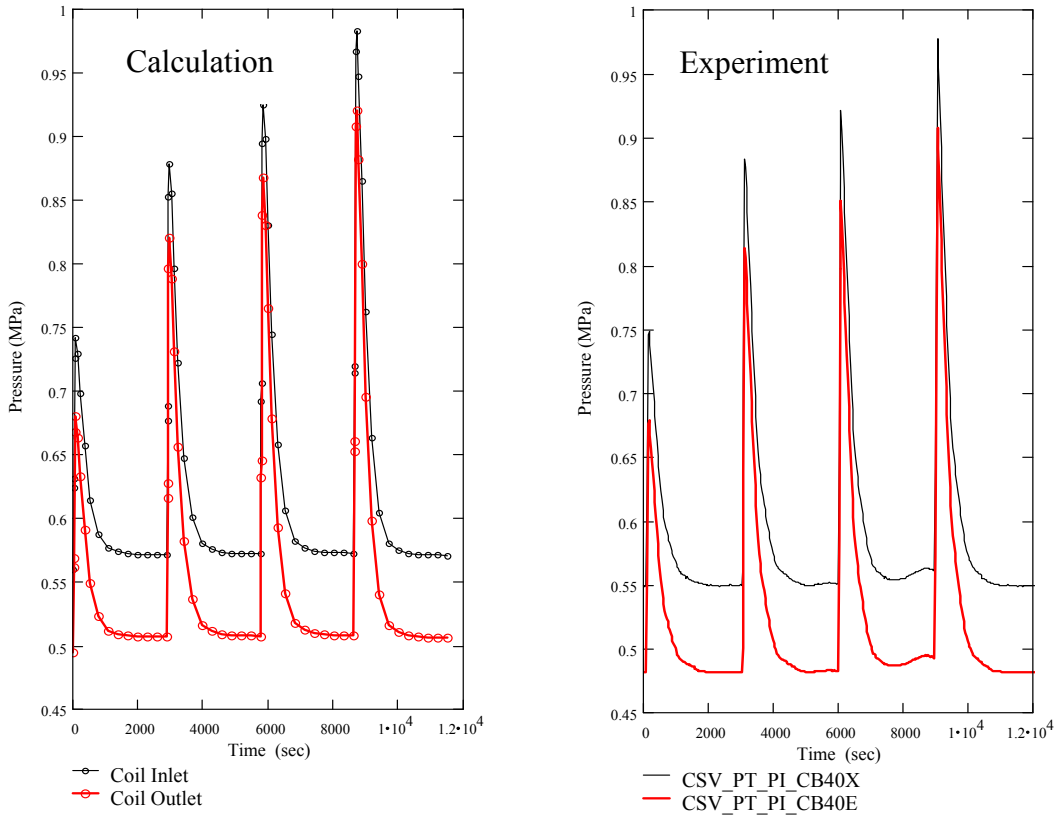

Figure 7. Evolution of the pressure at the inlet and outlet of CSMC for a series of current pulses with amplitudes of 30, 40, 43 and 46 kA.

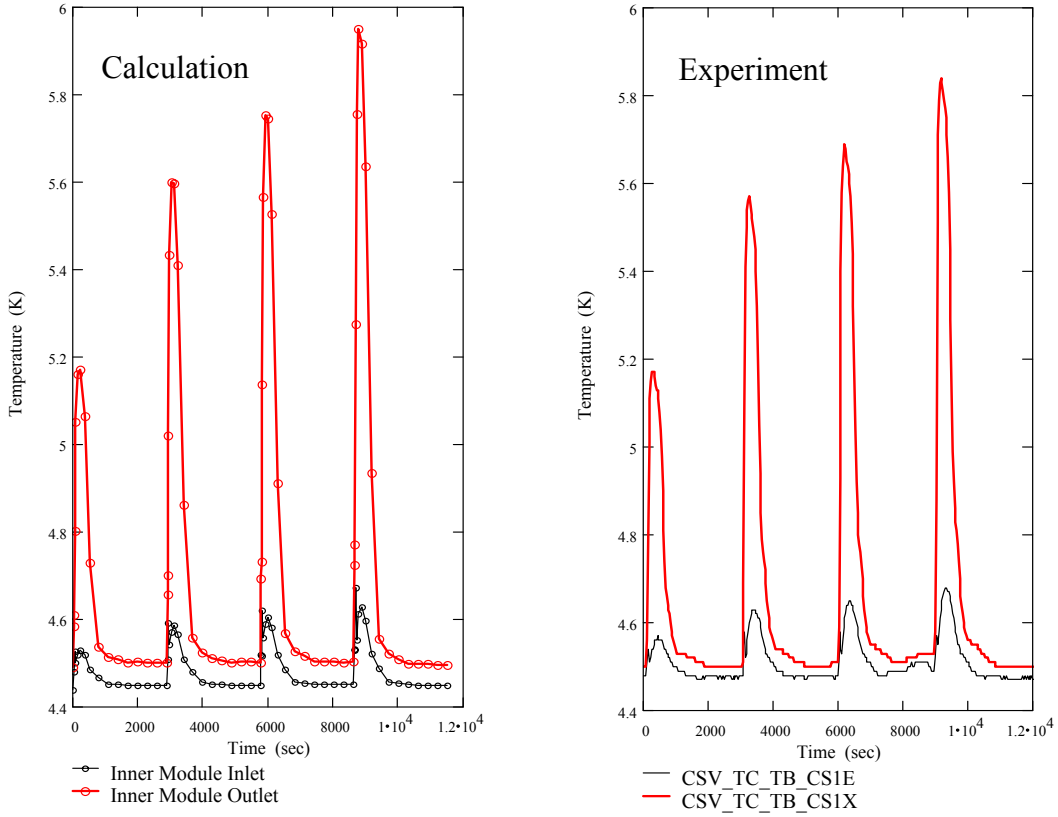

Figure 8. Evolution of temperatures at the inlet and outlet of the inner CSMC module for a series of current pulses with amplitudes of 30, 40, 43 and 46 kA.

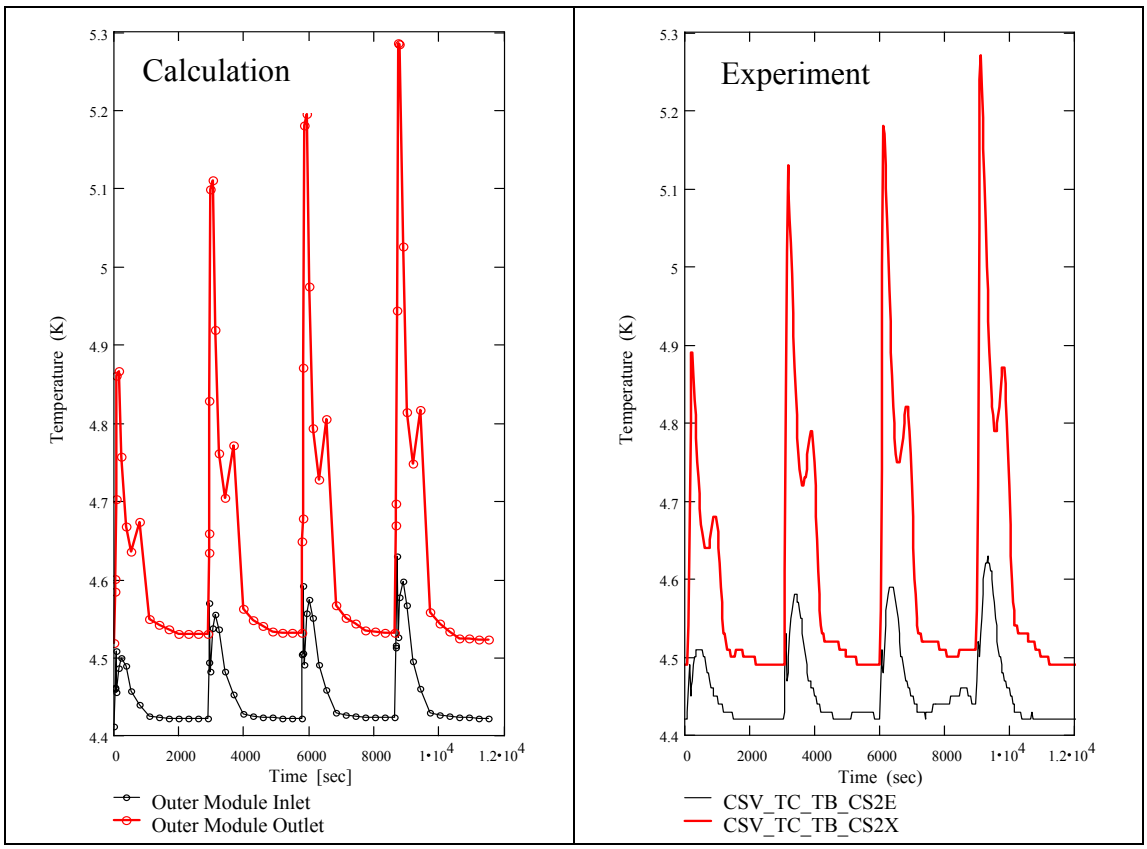

Figure 9. Evolution of temperatures at the inlet and outlet of the outer CSMC module for a series of current pulses with amplitudes of 30, 40, 43 and 46 kA.

The temperature evolutions at the inlet and outlet of the inner and outer CSMC modules are plotted in figures 8 and 9 for the same series of current pulses.

Figures 6 -9 show that the VINCENTA model ensures good accuracy for the integral transient cooling parameters, such as helium pressure and temperature, and proper evolution (time-history) of these parameters during current pulses and after them.

4.3 *Local parameters of transient helium flow for a series of current pulses*

Time variations in the temperature and helium mass flow rates at the inlet and outlet of each of 36 conductors are a manifestation of specific local parameters of the model depending on the thermohydraulic and electromagnetic characteristics of each conductor. The variations in the outlet temperature for twenty conductors 1A-10A and 1B-10B of the inner module are shown in figures 10 and 11 correspondingly. The evolution of the outlet temperatures for 11A-18A conductors of the outer CSMC module is shown in figure 12.

As mentioned above, the experiment has shown a difference between the outlet temperatures of A and B conductors of each winding layer. The maximum difference of about 0.75K occurs in the innermost layer of the inner CSMC module. This difference significantly decreases from the innermost layer to the outermost layers of CSMC.

A possible explanation of this fact is different hydraulic resistance of the supply pipes for conductors A and B. The impact of hydraulic resistance on mass flow rate is stronger in the internal winding layers because of a shorter conductor length.

It is also seen that the temperature profiles simulated for the conductor outlet slightly differ from actual profiles. A possible reason is the dependency of $n\tau$ on B and dB/dt (especially for the innermost layers), which was not taken into account in the present simulation.

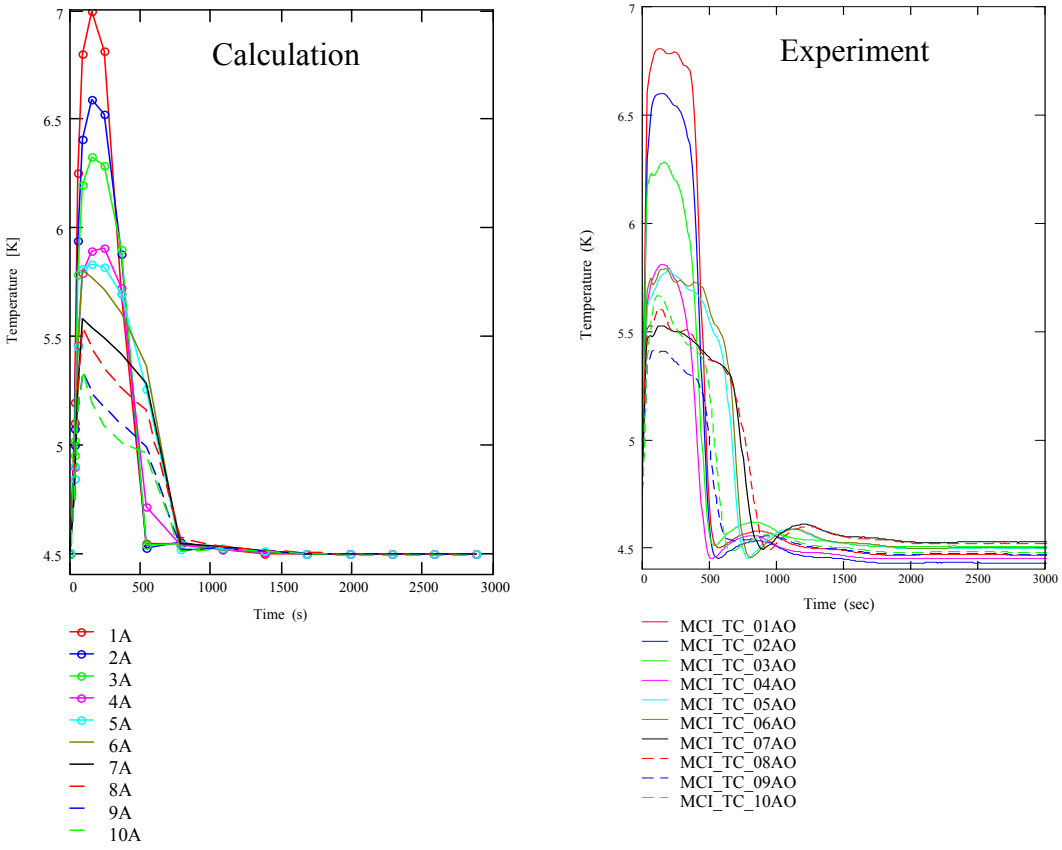

Figure 10. Evolution of temperatures at the outlets of 1A-10A conductors of the inner CSMC module for the 46 kA current pulse.

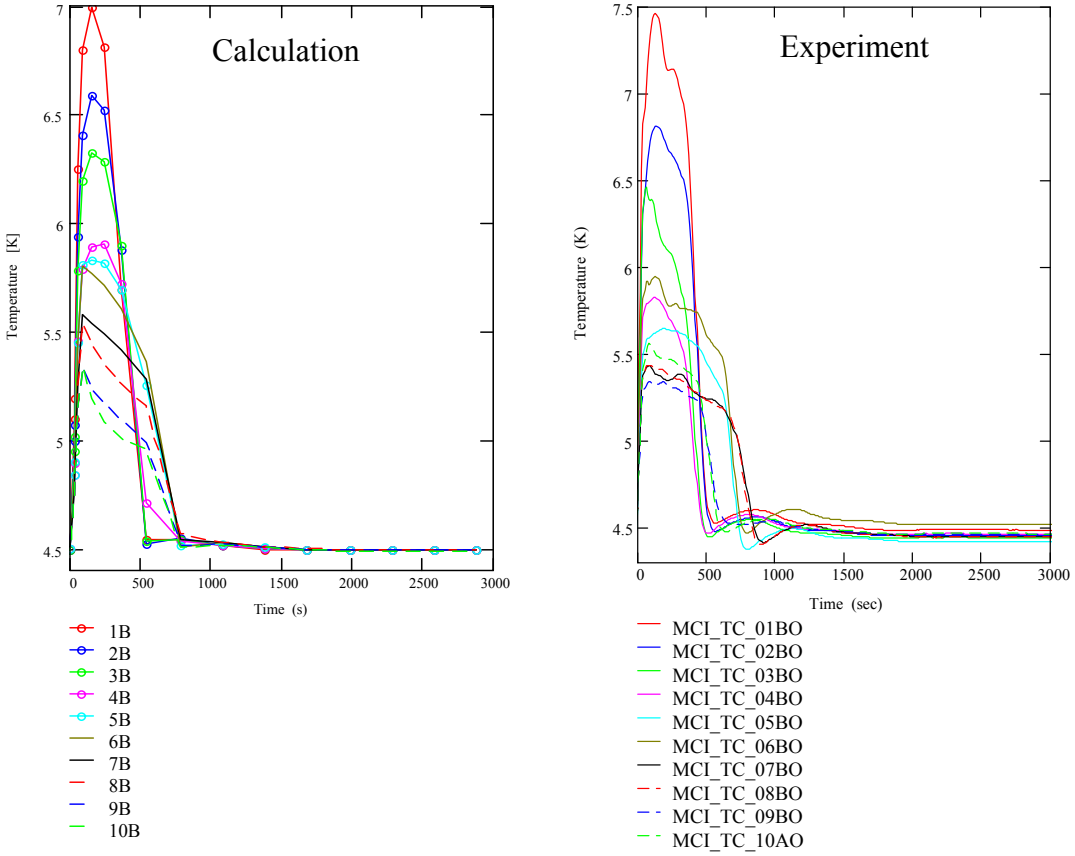

Figure. 11. Evolution of temperatures at the outlets of 1B-10B conductors of the inner CSMC module for the 46 kA current pulse.

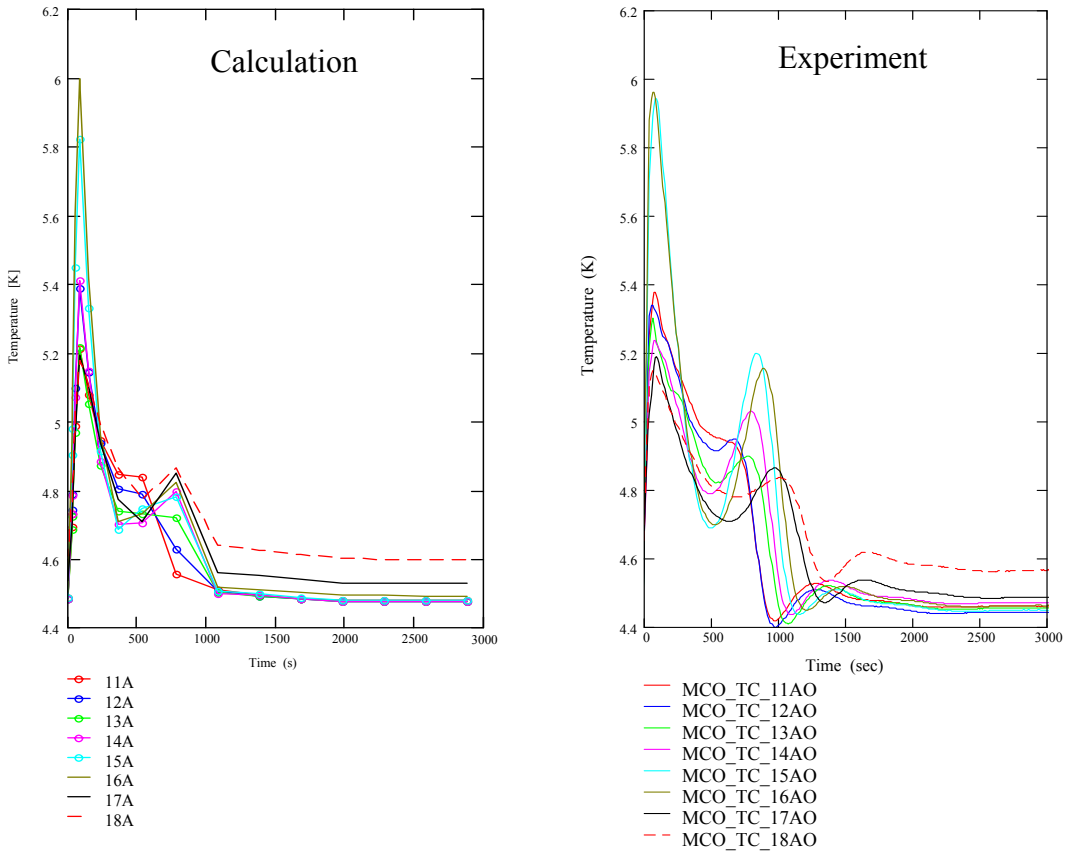

Figure 12. Evolution of temperatures at the outlets of 11A-18A conductors of the outer CSMC module for the 46 kA current pulse.

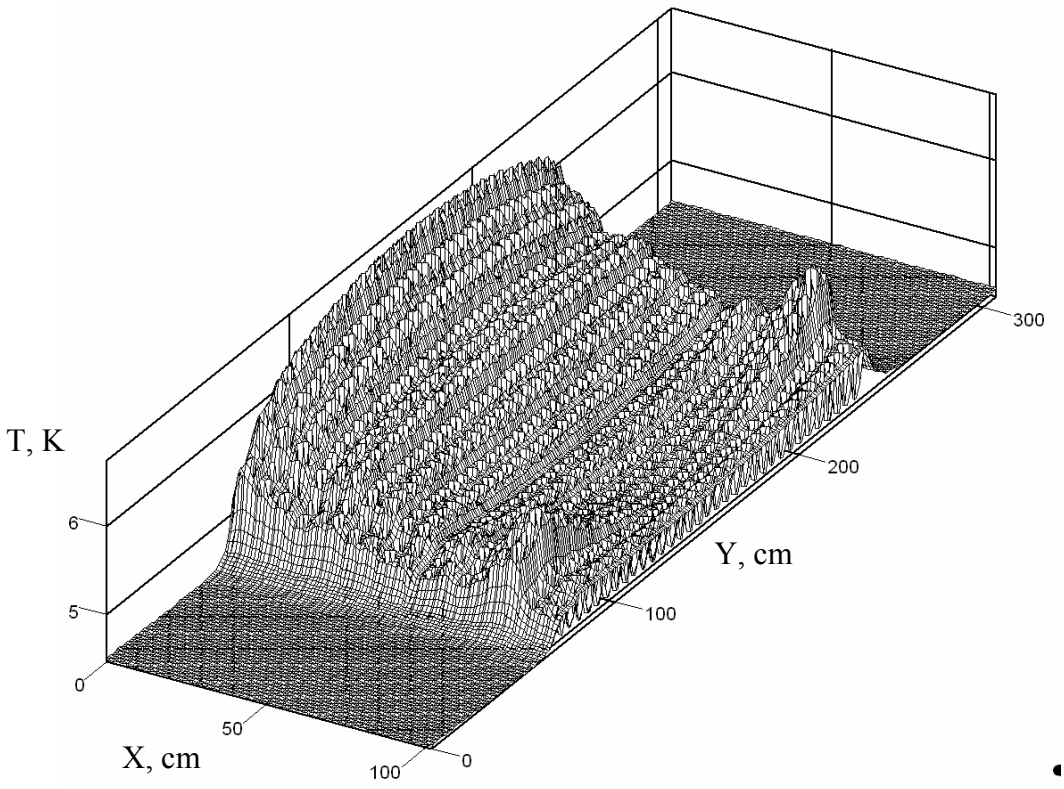

Figure 13. Temperature diagram for calculating the cross-section of the CSMC winding pack immediately after the end of the 46 kA current pulse.

Figures 10 -12 show that the VINCENTA model ensures good accuracy for the local cooling parameters of each conductor, including proper time histories of these parameters (only temperature shown as an example).

As no flow meters were installed at the conductor outlets, we could not compare the calculated flow rates with the data measured. . To illustrate the 2D modelling, the temperature diagram is shown in figure 13 for the cross section of the CSMC winding pack (including buffer zones) calculated just after the 46kA current pulse.

5. Conclusion

The comparison between numerical simulations and the CSMC experiment has shown that the VINCENTA model ensures good accuracy for the integral and local transient cooling parameters (helium pressure, flow rate and temperature) under a series of current pulses despite different magnitudes of the current at the flat top. The proper evolution (time-history) of transient cooling parameters could be found for each current pulse (30, 40, 43 and 46kA) even if the initial cooling parameters and AC losses were verified for only one current pulse with a flat top current of 46kA.

These results allow us to qualify the VINCENTA code as a reliable tool for modelling the magnet systems operating at high pulsed heat loads non-uniformly distributed over a winding pack.

The VINCENTA code can be recommended for modelling the active cooling control of the ITER magnet system that operates at high pulsed heat deposition due to variable electromagnetic losses and nuclear heat load. When using the active cooling control, the VINCENTA models facilitate careful monitoring of the local temperature of each conductor and checking whether its temperature is within the design limits.

Acknowledgments.

The authors are sincerely grateful to H. Takigamy, T. Kato, K. Hamada and E. Hara for the data presented and E. Zapretilina for useful discussions.